(Presented at the AAS/AIAA Astrodynamics Specialist Converence, Girdwood, AK, August 16-19, 1999)

AAS 99-355

A LIGHT-WEIGHT INFLATABLE HYPERSONIC DRAG DEVICE FOR VENUS ENTRY

Angus D. McRonald,*

Jet Propulsion Laboratory
California Institute of Technology

ABSTRACT

The author has studied inflatable drag devices (ballute = balloon + parachute) for deceleration in the atmosphere of Venus, for both direct aerocapture and for entry from circular orbit. The studies indicate that ballutes made of thin materials capable of temperatures of about 500 C allow an entry system mass that is , for both aerocapture and entry, less than with the conventional entry body. For aerocapture the exit conditions are controlled by measuring the velocity loss and releasing the ballute when the desired exit conditions are indicated. A development program is necessary to explore the ballute shapes and changes in flight and to mitigate possible instabilities. To design an entry vehicle using a ballute the designer takes the vacuum orbiter or the lander as it is on the surface, chooses one surface to attach the ballute, and places an MLI blanket on the other end.

PRIOR BALLUTE STUDIES

Ballutes seem to have been invented in the forties and fifties to reduce the ground impact speed of empty sounding rockets or rocket casings. The investigators probably discovered that the mass of a ballute, inflated at high altitude, to slow a returning high altitude sounding rocket was less than the mass of a necessarily stronger parachute system that would open at low Mach number and high pressure. In the late sixties studies and wind tunnel tests were performed (1,2) by Goodyear and NASA Langley with a view to using ballutes to assist deceleration of the Viking landers at Mars, but these ballutes were deployed after peak deceleration and heating, thus having limited potential to change the entry trajectory. A mushroom shape was found to be more stable than a sphere. In 1976 the authors of Ref. 3 proposed to use a ballute inflated prior to entry into Venus. They proposed a ballute of mass over 300 kg and computed the ablation during entry, and evaluated some candidate materials. In the mid eighties studies of ballute materials were done at Langley, but again the concept was to deploy ballutes after peak entry deceleration and heating. In recent

years NASA Ames has studied drag modulation of vehicles equipped with inflatable components (Ref. 4).

---

* A. D. McRonald is a Member of the Technical Staff at the Jet Propulsion Laboratory of the California Institute of Technology. The research described in this paper was carried out at the Jet Propulsion Laboratory, California Institute of Technology, under contract of the National Aeronautics and Space Administration.

RECENT STUDIES

In the past five years the author has studied the use of ballutes for aerocapture and entry at several planets, including a Mars orbiter and a Pluto lander, both reported in Ref. 5. Other applications not yet reported are ballutes at Neptune, Saturn, Jupiter, Titan and Earth. The present report describes ballutes applied to aerocapture at Venus of a sample return vehicle at direct entry, and to subsequent entry from a circular orbit after a plane change at a high apoapsis and aerobraking. (Ref. 6).

BASIC BALLUTE ENTRY

Entry using a large ballute dragged behind a payload reduces the entry convective heating rate to levels that can be radiated away thermally without ablation at surface temperatures on the order of 500 C, so that very thin balloon material can be used, inflated to a low pressure. For example, a ballute that has ten times the diameter of a payload package will have 100 times the area, thus experiencing peak heating at 0.01 of the atmospheric density value for a payload contained in a conventional entry vehicle. That is, the peak heating rate of the payload is now 0.1 of the prior value, and the peak heating rate on the ballute is about 0.03 of the prior payload value. Fortunately there is a material (Kapton) that can take 500 C temperature while retaining enough strength (5600 psi, Ref. 7) to function as a balloon, and there is a material (PBO = Polyboxoxazole, a liquid crystal polymer) that has a useful level of strength at 600 C to function as a net (Ref. 7).

BALLUTE SHAPES

The ballute concept is illustrated in Fig. 1. Although a ballute greatly reduces the peak convective heating (and also the radiative heating), there is only a small reduction in the peak g load due to drag, and therefore the ballute must be enclosed in a net that surrounds the ballute and communicates the total drag force to the payload. A ballute deployed from the rear of a payload, as illustrated in Fig. 1(a) has the advantage that the heating rate on the payload is reduced to the ballute level, but release of the ballute in aerocapture may not be easy. In Fig. 1(b) the ballute is let out on a tether, so that release is easy. Figure 1(c) shows a lens (or pancake) shape, which is more efficient than a sphere as a drag device, having a higher drag coefficient Cd (about 2 instead of 0.9)

and a smaller surface area (about half that of a sphere). Figure 1(c) can also be a disk with an outer ring, is similar to a lens in regard to drag area, but has even less material. For the lens and the disk one needs inflatable tubing deployed from the rear of the payload to help deploy the lens and disk ballute material in vacuum prior to entry. There is evidence (Ref. 8) that in conditions where a strong bow shock is formed ahead of the payload, there will be interaction with the bow shock of the ballute, leading to flow instability in the form of oscillations between different modes, perhaps sufficiently serious to invalidate accurate measurement of ballute drag. The remedy suggested is to have a ring ballute as in Fig. 1(d). Also, to avoid heating peaks at the edges (Ref. 9), the circular disk of Fig. 1(c) and the annular disk of Fig. 1(d) require inner and outer rings of diameter about 10% of the disk dimension, so that the mass of a ballute material in a disk with the necessary inner and outer rings will be about that in a lens , and this will be assumed in the mass calculations below.

AEROCAPTURE AND ENTRY

Figure 2 shows the delta-V loss in an atmospheric pass, as a function of the entry angle, for a number of ballutes with various values of B = m/CdA. The graphs of delta-V loss take the form of steep, almost straight lines. To aerocapture into a chosen orbit a certain delta-V is to be lost. For example, the exit speed at altitude 140 km for Venus is 10207 m/s just to capture into a long-period elliptic orbit, and is 7300 m/s for a close circular orbit. For an entry speed of 11500 m/s the corresponding delta-V losses are about 1300 and 4200 m/s. In the sample return case a delta-V loss of about 1500 +/- 100 m/s would be a suitable target. To perform aerocapture with a ballute one would choose an entry angle to give at least the minimum delta-V that one wishes for a complete atmospheric pass, allowing for error in delivery (i.e., entry angle error) and for difference between the assumed atmosphere and the actual atmosphere. For a given known entry mass m one evaluates trajectories with increasing size (decreasing B = m/CdA, where Cd is the drag coefficient and A is the frontal area). From the trajectory one can find the peak heating rate for a particular size of ballute, and from a radiative balance one finds the peak temperature that the ballute would experience. Presently available ballute materials have a peak temperature limit of about 500 C.

At the bottom Fig. 2 shows the entry angle range due to errors in the B plane (5 km) radius. One would choose a ballute large enough to keep the peak temperature below 500 C or so, and an entry angle that would give too much delta-V, even accounting for delivery and atmosphere errors, and then release the ballute at a measured delta-V that would give the desired exit speed for the orbiter after release.

For comparison, Fig. 2 shows on the right the delta-V parameters for conventional solid body aerocapture. The curves are shown for a body with lift/drag L/D ratio zero, and for steady upward lift for vehicles with L/D = 1 and 2, and downward lift for L/D = -1 (the L/D = -2 case is similar). These curves define an entry corridor. By entering about the center of the corridor, measuring the aero forces experienced, the vehicle can compute what L/D it must fly to the exit to emerge with the chosen delta-V. One can see that the entry angle for ballutes is about one half that for solid bodies. The major difference is in the stagnation pressure and the heating rate, which are very small for ballutes, while the g-loads are comparable, requiring the ballute to be enclosed in a net.

AEROCAPTURE CORRIDOR

The aerocapture corridors for the Venus ballutes are shown in Fig. 3, drawn for direct entry at V = 11.5 km/s at altitude 140 km, into a standard Venus atmosphere (Ref.9) The graphs of exit V for six ballutes, 1 to 6, of varying B, are steep lines which change at ballute release, shown at 10,300 m/s for all 6 ballutes and at 10,500 m/s for ballutes 4 and 6, becoming lines sloping moderately down to the right. By choosing the ballute size, the entry angle, the release velocity, and the B value of the orbiter after release, one can determine the exit V within acceptable limits.

AEROCAPTURE TRAJECTORIES

Aerocapture trajectories were computed for the six ballutes of Fig. 3 and with release at V = 10,300 m/s. Figure 4 shows the peak stagnation pressure, Fig. 5 shows the peak convective heating, qref, expressed relative to the stagnation point of a reference body with nose radius 0.43 m flying the same trajectory as the ballute, and then the orbiter after release. Fig. 6 shows the peak g-load, gmax, and Fig. 7 shows the added delta-V lost by the orbiter after ballute release. Fig. 7 also shows Qref, the time-integral of qref.

BALLUTE COMPONENTS

The ballutes computed here are assumed to have 5 components: 1) the drag disk of radius R (Kapton, 10 gm/m2 sheet), including the inner and outer rings, totaling about the same material as a lens (i.e., two surfaces) of the same diameter; (2) a net (PBO fibers) whose total cross sectional area must support the total peak drag force; a tensile strength of 56 kg/mm2 is assumed, and a length of 6R; (3) tubing (PBO) to be inflated to help the ballute material deploy to the desired shape in vacuum prior to the entry (assumed to be ten disk diameters in length, pressurized to 1 atm in 5 cm diameter tubing of thickness 2 mil, a thickness that gives 10 times the burst pressure cold, and equal to it when at 600 C); (4) an amount of pressurant helium gas sufficient to inflate the tubing to 1 atm and the rings of the disk to about 100 N/m2 (at least as great as the peak shock layer pressure); and (5) a He bottle of mass equal to that of the He. The tensile strength assumed for the net is the room temperature value; behind the ballute the net is shielded from stagnation heating, and in front it is assumed that the net material is shielded by the tubing or in some other way. The materials of the ballute were assumed to be either 10 or 20 gm/m2 Kapton, or 20 gm/m2 of PBO. The relative mass of the components varies with the ballute radius, R. The tubing and the net vary as R, the net varies also as gmax and m, the ballute fabric mass varies as R squared, and the He mass varies as R in the tubing and as R squared in the lens or rings. It turns out that the He gas mass is relatively small, and only the three main components - ballute, net and tubing will be significant here. Six values of m/CdA were computed, and for each of these values one can vary m and thus R, so that the fraction of mass required for the ballute and its components varies with the assumed entry mass, m.

BALLUTE MASS

Since the governing parameter for a ballute trajectory is B = m/CdA, it is useful to begin with a simple mass of 100 kg and a chosen B = 1 kg/m2, for example. Then, with Cd = 2 for a disk or lens, and A = the area of the circle, one can find the corresponding radius R. From the value of qrefmax one can compute the peak ballute heating and the equilibrium radiative peak temperature, Tmax, and then find a ballute B value that brings Tmax below 500 C (773 K). Thereafter one can increase A to suit the desired entry mass m. The basic ballute mass components (excluding He gas bottle, ballute release device, ballute cover or container) are shown in Table 1 for representative Venus direct entry at Ve140 = 11.5 km/s and m = 100 kg.

Table 1. Ballute for Direct Venus Aerocapture, Ve140 = 11.5 km/s, based on 100 kg entry mass

B=m/CdA,kg/m2	1	0.5	0.25	0.10	0.05
Radius R, m	4.0	5.66	8.0	12.65	17.89
Entry angle, deg	3.8	3.8	3.5	3.0	3.0
pmax, N/m2	101	87	22	13	10
qrefmax,W/cm2	27.0	22.7	12.7	9.2	7.6
gmax	5.29	9.13	4.53	6.7	10.94
mass of lens,kg 1.11	2.22	4.44	11.11	22.13	
mass of net, kg 0.34	0.83	1.06	1.36	2.19	
mass of tubing, kg	1.24	1.75	2.47	3.92	5.55
mass of He,rings	.0035	.0083	.0278	.1098	.3104
mass of He,tubing	.0356	,0503	.0709	.1125	.1593
total mass,kg	2.75	4.86	8.07	16.61	30.34
(excluding He bottle and fittings)					
Tmax, degK	1219	1025	849	740	675
Tmax,deg C	946	752	576	467	402

These masses and the values of R are for an entry mass m of 100 kg nominal. They scale as: area with m, lens mass with m , net mass with m and R, tubing mass with R, He mass with m for rings and R for tubing.

CIRCULAR ORBIT ENTRY

Trajectories were computed for entry angles of 1.5, 2.0, 2.5 and 3.0, at altitude 140 km, at an entry speed of 7217 m/s, for six ballute sizes (B= 1., 0.5, 0.25, 0.10, 0.05, and 0.025 kg/m2. Table 2 shows parameters for an entry angle of 2 deg, for six ballute sizes and also for a typical solid entry body with B = 60 kg/m2. It can be seen that the ballutes have much smaller peak pressure and peak heating (the qref values are approximately the value for a payload package, since the reference radius 0.43 m is comparable with that of the payload, the ballute rate will be considerably less), and decelerate much higher in the atmosphere, and with a much smaller range (from the entry point to the point with V= 100 m/s). We note that the peak g-load is similar, communicated to the payload via the net enclosing the ballute. For example a payload on a ballute with B = 0.10 kg/m2 has peak pressure reduced by about 700 times, and peak heating reduced about 30 times, compared to the payload entering in a typical solid body. It may be significant that the range is down by about a factor of 2, since one would expect the footprint to be less also.

Table 2. Venus Circular Orbit Entry Ballute Parameters.

Ve140 =7217 m/s, entry angle at 140 km = 2.0 deg

B=m/CdA, kg/m2	pmax max W/cm2	qref	gmax	Range, km	Qref J/cm2	peak heating density kg/m3	speed m/s	altitude km	altitude at 100m/s km
1.0	240	9.7	12.5	983	608	.35(-5)	6080	112	88
0.5	119	6.8	12.4	905	427	.18(-5)	6011	114	91
0.25	59	4.77	12.4	825	299	.86(-6)	6056	118	93
0.10	23.3	2.95	12.1	720	184	.317(-6)	6095	122	96
0.05	11.4	2.07	11.9	640	126	.154(-6)	6107	124	99
0.025	5.46	1.47	11.5	561	85	.763(-7)	6120	128	101
60 (solid)	15400	82	13.1	1435	4715	.238(-3)	6125	96	68

VENUS BALLUTE MASSES

From the trajectory data for direct hyperbolic entry and for the entry from circular orbit , given an entry mass, one can evaluate the ballute radius and hence the peak radiative equilibrium temperature. The peak temperature, Tmax, is shown in Fig. 8 for entry masses of 100 and 400 kg, and also for specific Venus Sample Return masses (Ref. 9) of 2065 and 3000 kg for direct entry, and 500 and 1100 kg considered for entry from circular orbit. Values of Tmax are shown for two values of the ballute material emissivity, 0.5 and 0.7, believed to bracket the true value for films of the thickness considered here, 7 to 14 micron (10 to 20 gm/m2).

The ballute mass, determined from the components shown in Table 1, is shown in Fig. 9 as a function of ballute and radius and as a fraction of entry mass for entry mass of 100, 400, 2065 and

3000 for direct entry, and for mass of 500 and 1000 kg for entry from circular orbit. Two ballute thicknesses, 10 gm/m2 and 20 gm/m2 are shown.

From Fig. 8, choosing a Tmax, e.g., 500 C for Kapton, one can evaluate the ballute radius for the appropriate entry mass, and from Fig. 9 one can evaluate the mass fraction = ballute system mass/entry mass for that temperature and mass. Trajectories were also computed for a direct entry of an atmosphere sample taken at low speed in the upper atmosphere without descent to the surface. The trajectories are similar to the surface sample aerocapture entry, but the ballute is not released. Data similar to those shown on Figs. 8 and 9 were prepared. The outcome is shown in Table 3, where the somewhat steeper entry calls for a slightly larger ballute and somewhat greater net force. than in case 1. Trajectories were also computed for a fourth ballute for hyperbolic flythrough to return an atomized atmosphere sample. The entry mass was 800 kg and the entry angle is more shallow than case 1, so that the ballute is smaller and has a smaller mass fraction than the surface sample return case.

The outcome for four ballutes is shown in Table 3.

Table 3. Venus Sample Return Ballutes: Mass Fractions

Mission Item

1. Surface sample, direct entry 2. surface sample, entry from circular orbit
3. air sample, direct entry to low speed 4. hyperbolic flythrough, atom sample

	1	2	3	4
Entry speed, km/s	11.5	7.217	11.5	11.5
Entry mass, kg 2491	1067	1960	800	
ballute mass density, gm/m2	10	10	10	10
Tmax, deg C	500	500	500	500
emissivity	0.5	0.5	0.5	0.5
radius, m	33	12	35	13
mass fraction, %	6.3	3.4	7.0	1.1
mass, kg	157	37.4	137	9
assumed mass, %	15	11	15	15
assumed mass ,kg	448	117	294	120
ballute actual % of allocation	35.0	32.0	46.6	14

FLOW FIELD STABILITY

Reference 8 has indicated that a disk or lens form ballute (Fig.1) will show interaction between the bow shock from the front payload body and the bow shock of the rear ballute body, in conditions where the payload shock is substantial. The remedy suggested is to have a ring or doughnut ballute shape. It is appropriate then to consider the Knudsen number of the payload during aerocapture and entry. The mean free path of the free stream is shown in Fig. 10, and this can be interpreted as about the Knudsen number of the payload, as it is likely to have a diameter of about 1 m. It is normally accepted that a Kn of 0.01 is necessary for a developed bow shock, and Fig. 10 shows that in the aerocapture case the ballute is released before this value is reached. In the entry case however, much of the drag occurs in developed continuum conditions, and a ring shaped ballute is indicated. One way to determine how large a hole the doughnut should have is to fly ring ballutes with different hole sizes on a sounding rocket, to be deployed when in vacuum before reentering the atmosphere, and record the behavior on accelerators and with a camera. Conceptually the length of the tubing and net strands to the inner rings will be chosen so that the drag force tends to keep the ballute in the correct shape, even if the tubing disintegrates A final test with actual high-speed real gas conditions should also be done to demonstrate that one has a stable ballute functioning as predicted here. A thermal analysis of the system should be done. For aerocapture one is likely to find free-molecular conditions on the thin tubes used for deployment, which may also carry the strands of the g-load net, and to find continuum conditions on the ballute, while the payload body is in an intermediate regime. For an entry ballute similar conditions will be met briefly, and then all

three objects - ballute, payload and tubing - will move towards continuum flow conditions. The consequences for heating are important. For example, the small objects (tubing and net strands) will have a heating limit at the low density for aerocapture, but not at later entry conditions during entry.

BALLUTE MATERIAL DATA

The available data on strength versus temperature (Ref. 4) for Kapton and PBO seems to leave some questions unanswered. Kapton is available in films commercially down to thicknesses at or below the 7 micron (10 gm/m2) proposed here, and PBO is available commerically as fibers, and can be made in film form in limited quantities, with varying thickness in the range 10-30 gm/m2. Ref. 4 gives graphs for the tensile strength of PBO film and Kapton film (in the machine direction), and some values are shown in Table 5. In this paper the net, made of PBO, was evaluated with a cold strength of 56 kg/mm2, and the ballute fabric was assumed to be Kapton, 7 micron film with strength 5.6 ksi (3.943 kg/mm2) at 500 C. Ref. 4 gives a table comparing material properties, listing PBO with tensile strength of 56-63 kg/mm2, and gives a curve in the machine direction with the values of Table 4, as well as a strength of 820 ksi (576 kg/mm2) for high performance PBO fiber.

Table 4. Ballute Film Strength Versus Temperature.

Temperature	Tensile strength, ksi and (kg/mm2)			
deg C	Kapton film	PBO film (machine direction)	General PBO film	High performance PBO fiber
20	30.0 (21.1)	140 (98.4)	(56-63)	820 (576)
100	22.5 (15.8)	120 (84.4)		
200	15.3 (10.8)	90 (63.3)		
300	11.0 (7.7)	70 (49.2)		
400	7.9 (5.55)	65 (45.7)		
500	5.6 (3.94)	44 (30.9)		

It would seem that one could find high-performance PBO fibers for the ballute net that would be much stronger than the 56 kg/mm2 assumed in this paper.

COMPUTED TEMPERATURES

The reference heating rate quoted here is a simple approximation for the stagnation level of a sphere in air. Ref. 10 has done an analysis of a sphere and a disk for the peak conditions at Venus direct entry aerocapture, and finds a peak heating rate of 1.3 W/cm2 for a ballute of radius 50 m, and then a peak temperature of 712 K, based on a one-sided radiation with emissivity 0.9. The corresponding heating rate for this radius evaluated with the simple correlation is 1.26 W/cm2, and

the assumption of emissivity 0.5 on two sides gives a Tmax of 686 K For a disk with rings (would include a lens) Ref. 10 finds a heating level of 0.46 W/cm2 (Tmax = 550 K) at the center, and a peak of 0.73 W/cm2 (Tmax = 615 K) at a shoulder assumed to be of radius 5 m. The value taken in the present paper is the same as for a sphere, so that the disk or lens temperatures evaluated may be high by 60 deg, equivalent to a heating factor of about 1.6. Incidentally, the free-molecular heating for the maximum continuum point above is 2.6 W/cm2, so that the heating rate will be small for small items and for large items, and greater for items of intermediate size in the free stream.

DISCUSSION

Table 1 shows the component masses for an entry of 100 kg, and Table 3 shows an entry mass of 2500 kg with a radius of 33 m. To evaluate the component masses of the 33 m ballute we scale up a mid-sized ballute from Table 1, e.g. R = 8 m. The radius is to be scaled up from 8 to 33 m, about 4 times, and the mass m has to be scaled up from 100 to 2500 kg, about 25. The ballute fabric scales as R squared, about 16, the net scales as m (25) and R(4), i.e., about 100, and the tubing scales as R, about 4. Then we have the values of Table 5.

Table 5. Components of the Venus entry aerocapture ballute.

Entry mass	radius,m	mass, kg			
		ballute material	net	tubing	total
100 nominal	8	4.44	1.06	2.47	8.07
2500	33	75.5	109.3	10.2	195

whereas the graph interpolations of temperature and radius gave a total of 157 kg. However, we can see that m up 25 R up 4.125 the ballute material is 75 of 195 (38%), the net is 109 of 195 area up 17.0 (55.9 %) and the tubing is 10.2 of 195 (5.2 %). The He gas mass stays small.

Of these components the basics, derived from the trajectory parameters, are the fabric and the net, while the tubing mass is entirely assumed; however, for the large ballutes called for in the large mass Venus entries the tubing becomes a small part of the total. With no margin on the basic ballute fabric and the net (the latter evaluated on the basis of the room temperature tensile limit) the masses of the aerocapture ballute and the circular orbit entry ballute are computed to be about one third of the assumed values (15 % and 11 %). Allowing the computed mass to double when one includes packaging, reduced strength with heating and exposure, a device to release the ballute, etc, the estimated mass of ballutes 1 and 2 of Table 2 are about 10.5% and 7.0 %, compared with the assumed values of 15 and 11 %. It should be noted that some of the assumptions are conservative, e.g., the strength of the PBO net and tubing may be more than the 56 kg/mm2 assumed (see Table 5), and the drag coefficient of 2.0 for the lens or disk may be small (for a sphere Ref. 10 found 1.24, compared with 0.9 assumed here). On the other hand some items are omitted, e,g, explosive bolts to release the ballute, a cover or container to hold the stowed ballute, an accelerometer package to control ballute release, but these are probably covered by the factor of 2 suggested here between the basic mass and the probable mass.

Data on the heat shield and structural mass of conventional Venus entry vehicles is not available. The Pioneer-Venus entry probes were designed to enter at steep angles, and so had much more structural mass than a vehicle would require for aerocapture. Similarly, the Pioneer-Venus probe heat shield was designed to accept much higher heating levels, and should not be compared. One would guess that new materials and a light construction adapted to the immediate task would allow

the structure and heat shield mass fraction for Venus sample return entry vehicles to be in the vicinity of 20-25 % of the entry mass, i.e., considerably above the present indications for ballutes.

CONCLUSIONS

This study of ballutes for a Venus Sample Return mission indicates that ballutes can be designed to operate at temperatures on the order of 500 C and under the g-loads encountered in aerocapture at Venus, in direct entry as if to land, and during entry from a circular orbit, and that the mass of the ballute system will probably be lower than the somewhat arbitrary 15% and 11% assumed in Ref. 7 for aerocapture and circular orbit entry, respectively. For ballutes to be ready for project use a development program must be followed to experimentally validate concepts for packaging and storing a large ballute for months, deploying it reliably in a matter of minutes prior to planetary entry, proving that the aerodynamic behavior is stable and predictable, and releasing it under the control of a reliable accelerometer integrator system. The study indicates that aerocapture and entry using ballutes enables a payload to be placed in orbit or to land without being included in a conventional entry vehicle with heat shield.

REFERENCES

1. I.M.Jahemenko,"Ballute Characteristics in the 0.1 to 10 Mach Number Speed Range", J. Spacecraft, Vol. 4, No. 8, 1058-63, August, 1967.
2. L. D. Guy, "Structural and Decelerator Design Options for Mars Entry", J. Spacecraft, Vol. 6, No. 1, 44-49, January, 1969.
3. H. Akiba et al., "Feasibility Study of Buoyant Venus Station Placed by Inflated Balloon Entry", Paper at the 27th Int.Conf. Astronomy, Anaheim, Calif., October, 1976.
4. M.Murbach, NASA Ames, Private Communication, May 1999.
5. A.McRonald, "A Light-Weight Inflatable Hypersonic Drag Device for Planetary Entry", Paper at the Association Aeronautique de France Conf. at Arcachon, France, March 16-18, 1999.
6. T. Sweetser et al., "Venus Surface Sample Return: A Weighty High-Pressure Challenge", Paper at the AAS-AIAA Conf. in Alaska, August 1999.
7. A. Yavrouian et al., "High Temperature Materials for Venus Balloon Envelopes", AIAA Paper, 1995.
8. H. Hornung, California Institute of Technology, Private Communication, June 1999.
9. A.Kliore,"The Venus International Reference Atmosphere", Advances in Space Research, Vol. 5, No. 11, 1986.
10. P.Gnoffo, NASA Langley, Private Communication, June 1999.

ACKNOWLEDGEMENT

The author gratefully acknowledges support from many JPL colleagues involved in mission design and technology development, e.g., Bob Miyake, Jim Cutts and Jeff Hall.

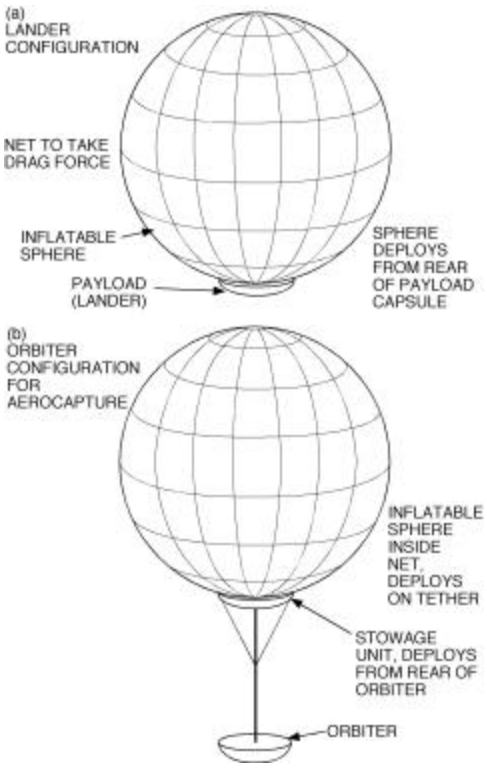

Fig. 1 Ballute configurations:

(a) Lander configuration
(b) Orbiter configuration

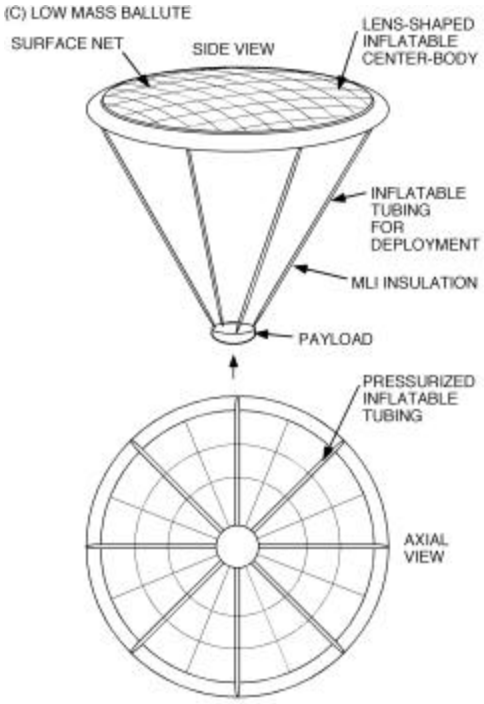

(c) Lens or Disk ballute

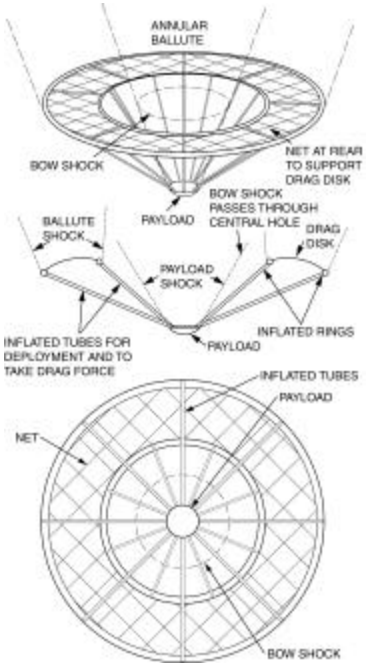

(d) Annular or Ring ballute

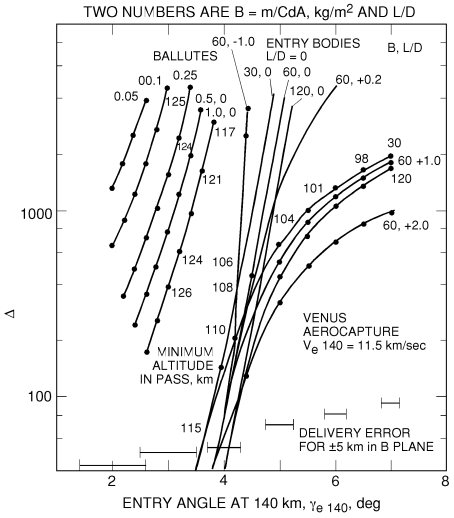

Fig. 2 Delta-V loss in an atmospheric pass versus entry angle, for ballutes and lifting bodies, Venus entry.

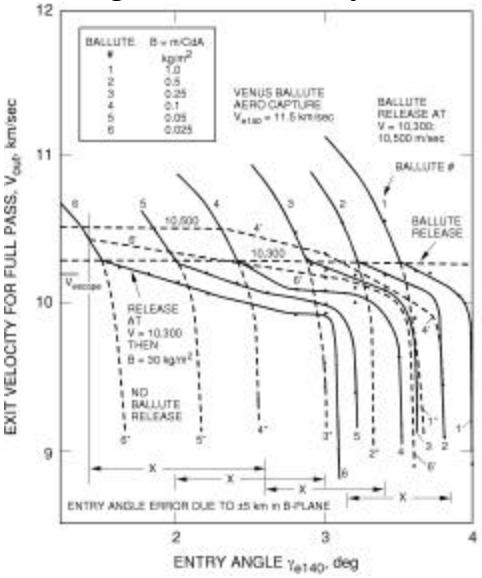

Fig. 3. Ballute exit velocity versus entry angle, with and without release, Venus direct entry.

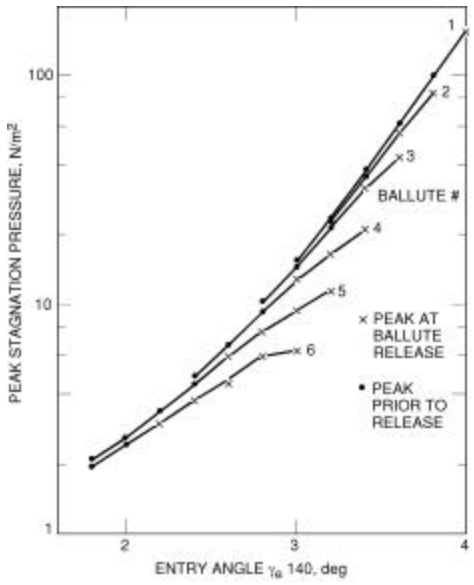

Fig. 4. Peak stagnation pressure versus entry angle, Venus direct entry.

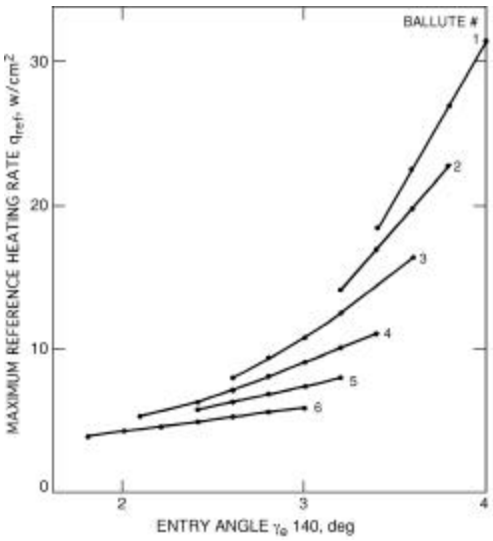

Fig. 5. Peak reference convective stagnation point heating versus entry angle, Venus direct entry.

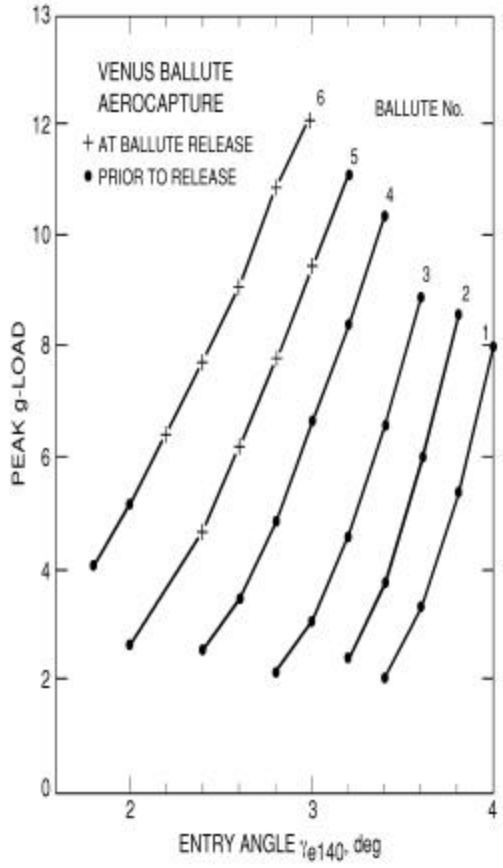

Fig. 6. Peak g-load versus entry angle, Venus direct entry.

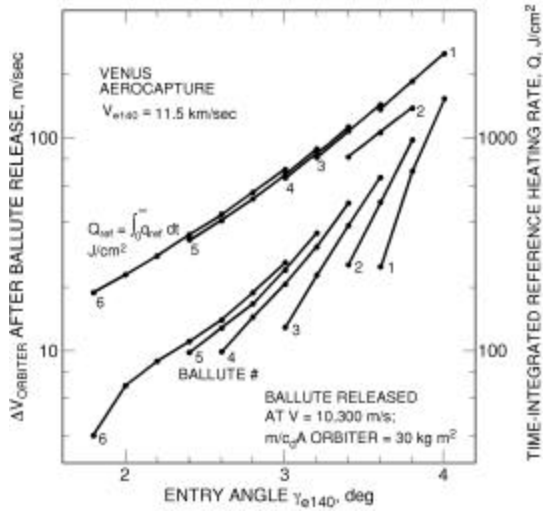

Fig. 7. Delta-V loss by orbiter after ballute release versus entry angle, and time-integrated reference heating.

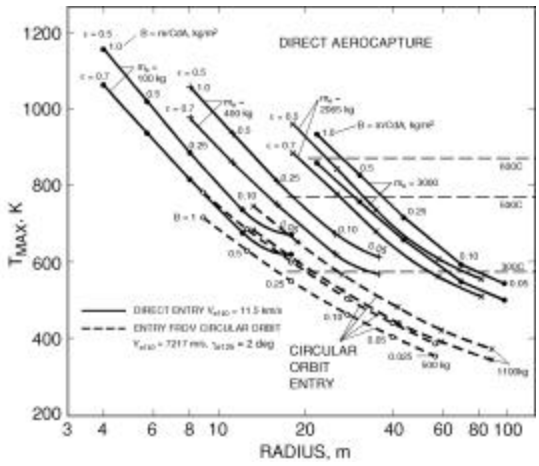

Fig. 8. Peak ballute temperature versus radius for several entry masses, Venus direct entry and circular orbit entry.

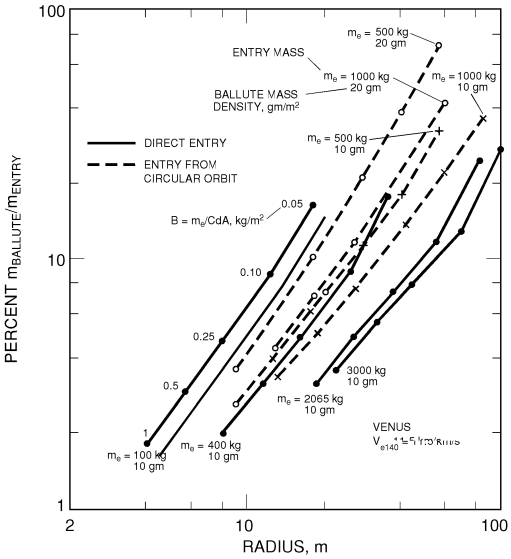

Fig. 9. Ballute mass fraction (ballute mass/entry mass) versus radius for several masses, Venus direct entry and circular orbit entry.

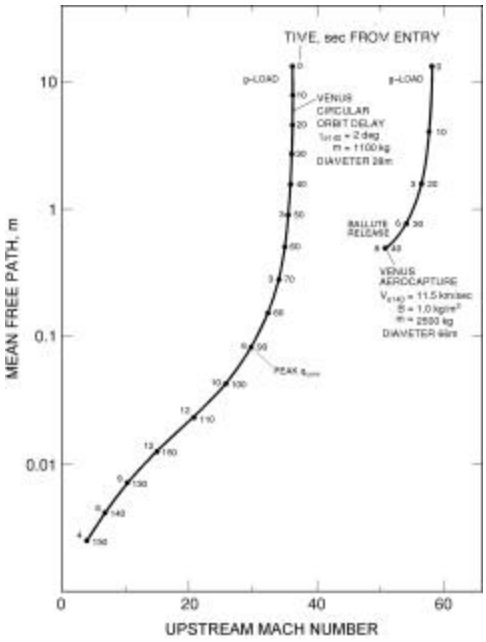

Fig. 10. Mean free path versus Mach number for typical ballute entry into Venus, direct and circular orbit entry.